Numerical studies of the glass transition in the roughness of a crystalline surface with a disordered substrate

1996 J. Phys. A: Math. Gen. 29 21

(http://iopscience.iop.org/0305-4470/29/1/006)

J. Phys. A: Math. Gen. **29** (1996) 21–32. Printed in the UK

Numerical studies of the glass transition in the roughness of a crystalline surface with a disordered substrate

D Cule and Y Shapir

Department of Physics and Astronomy, University of Rochester, Rochester, NY 14627, USA

Received 29 June 1995

Abstract. We investigate by extensive Monte Carlo simulations the discrete Gaussian model for a crystalline surface on a disordered substrate. The average height–height correlation $C(L) = \langle (h(\vec{x}) - h(\vec{x} + \vec{L}))^2 \rangle$ scales as $A(T) \ln L$ at all temperatures. A transition is observed in the temperature dependence of the coefficient $A(T)$: while $A(T) \sim T$ for $T > T_c$ it becomes almost temperature independent below T_c. This behaviour is consistent with the predictions of a replica-symmetry broken solution of the Gaussian variational calculations. We also explore the probability distribution $P(q)$ of a quasi-overlap q. It exhibits a transition at T_c with its maxima shifting away from $q = 0$. The size-dependence of the ratio of the fourth to second moment yields a first estimate for the correlation-length exponent $\nu \approx 1.23$, and for the dynamic exponent at T_c: $z \approx 2.3$.

1. Introduction

Surface roughening has been studied extensively both theoretically and experimentally. The basic mechanism is well understood [1, 2]: at low temperature the crystalline surface is essentially flat. At temperature $T > T_R$, where T_R is the temperature of the roughening transition, the surface is rough. This is reflected in the height–height correlation function $C(L) = \langle (h(\vec{x} + L) - h(\vec{x}))^2 \rangle$. Below T_R, $C(L)$ approaches a constant at long distances L while above T_R its asymptotic behaviour is $C(L) \sim T \ln L$. This behaviour may be understood from the competition between energy and entropy: at very low temperature the energy is minimized when the surface is parallel to the substrate. At $T > T_R$ the entropy dominates, the step free-energy vanishes and the periodic potential is irrelevant.

A natural question then arises [3]: what will be the effects of disorder in the substrate at low temperature? The behaviour for $T < T_R$ depends on the rigidity of the crystal. If the rigidity is finite the crystal will be affected by the substrate disorder only close to the substrate. There will be some 'healing' distance beyond which the periodic crystal will not be sensitive to the disorder in the substrate. If the height exceeds this distance the behaviour of the surface will be the same as if the substrate were flat.

Here we study the behaviour of the substrate when the height is much smaller than the 'healing' distance, which we assume to be infinite (as it is in the case of an infinite rigidity). We find a new behaviour in which the surface remains rough at low temperature but the roughness is due to the disorder (rather than the temperature) and has glassy properties. (If the height is of the order of the 'healing' distance, a crossover between the two behaviours will occur as the surface height grows. This crossover will be addressed elsewhere.) A brief summary of the important results concerning the equilibrium properties was given in our earlier publication [4].

0305-4470/96/010021+12$19.50

The organization of the paper is as follows. In the next section the discrete Gaussian model with the disorder is described and the results of previous studies of the related random-phase sine–Gordon model (RSGM) are reviewed. In section 3 the numerical simulations are presented and discussed. The last section 4 is devoted to the conclusions.

2. The random discrete Gaussian model

Let us denote the height of the surface above a point i on the 2D basal lattice by h_i. The so-called discrete Gaussian model which was very successful in describing the surface of a crystal on a flat substrate [1, 2] is given by the Hamiltonian

$$H = \frac{\kappa}{2} \sum_{\langle i,j \rangle} (h_i - h_j)^2 \tag{2.1}$$

where κ is the surface tension, and the sum runs over nearest-neighbour pairs. If the substrate is flat the variables h_i are always equal to $n_i b$ where b is the vertical lattice spacing and n_i is an integer. If the substrate is disordered we have to add (or subtract) the height of the substrate itself D_i (with respect to some reference height $h = 0$). The deviations in the substrate affect the surface only to the extent to which they deviate from an integer multiple of b. Therefore, the relevant quantity is $d_i \equiv D_i \,(\mathrm{mod}\, b)$. Without loss of generality we can therefore assume that the local deviations are d_i and that they are restricted to the interval $(-b/2, +b/2]$. If the substrate is totally random d_i will be uniformly distributed in this interval. We also assume that d_i on different sites are uncorrelated keeping in mind that the conclusions will also apply in the presence of short-range correlations in the substrate height. The height variable h_i then takes the values $h_i = d_i + n_i b$ where n_i is any, positive or negative, integer (see figure 1).

The partition function for a given realization of the disorder consists in summing $\exp\{-\beta\mathcal{H}\}$ over all possible integers n_i. Using the Poisson summation formula:

$$\sum_{n_i=-\infty}^{\infty} \delta(h_i - d_i - n_i b) = \frac{1}{b} \sum_{m_i=-\infty}^{\infty} \mathrm{e}^{2\pi \mathrm{i}(h_i - d_i)m_i/b} \tag{2.2}$$

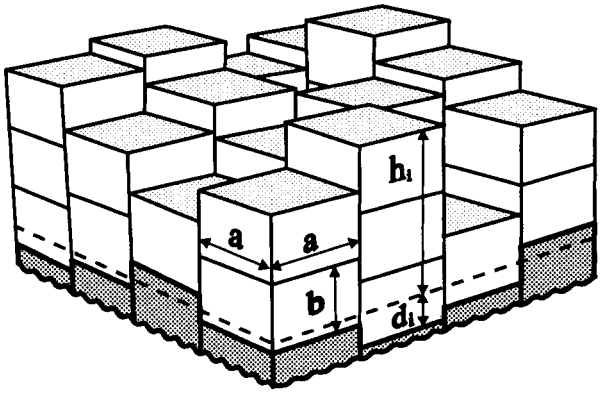

Figure 1. Schematic illustration of the simulated model. The heights h_i are measured with respect to the flat reference surface denoted by broken lines. The shaded area on the bottom indicates the disorder substrate.

and introducing continuous fields ϕ_i, the partition function may be expressed as

$$Z = \left(\prod_i \int_{-\infty}^{+\infty} \mathrm{d}\phi_i \right) \sum_{m_i=-\infty}^{+\infty} \exp \left\{ -\frac{\kappa\beta}{2} \sum_{\langle i,j \rangle} (\phi_i - \phi_j)^2 + \sum_i 2\pi \mathrm{i} \, (\phi_i - d_i) \, m_i / b \right\} . \tag{2.3}$$

To reach the continuum limit ϕ_i are replaced by $\phi(\vec{x})$, and finite differences are replaced by the derivatives. Near the critical point only the first harmonic in ϕ is relevant [1]. The RSGM Hamiltonian is obtained by neglecting the higher harmonics:

$$Z = \int \mathrm{d}\vec{x} \int_{-\infty}^{+\infty} \mathrm{d}\phi(\vec{x}) \, \exp \left\{ - \int \mathrm{d}\vec{x} \left[\frac{\kappa\beta}{2} \left[\nabla\phi(\vec{x}) \right]^2 - \lambda \cos \left(2\pi \left[\phi(\vec{x}) - d(\vec{x}) \right] / b \right) \right] \right\} \tag{2.4}$$

where $\lambda \sim 1$. The horizontal lattice spacing was chosen as $a = 1$.

The most important quantity to explore is the averaged height–height correlation function:

$$C(\boldsymbol{r}) \equiv \left[\left\langle \overline{(h(\boldsymbol{r} + \boldsymbol{r}_0) - h(\boldsymbol{r}_0))^2} \right\rangle_T \right]_{av} . \tag{2.5}$$

Here and throughout this paper $\langle \cdots \rangle_T$ denotes a thermal average (in the MC procedure it corresponds to an averaging over 'time' or MC steps). $[\cdots]_{av}$ denotes an average over disorder; in the MC procedure it is performed by averaging over different realizations of the d_i (sometimes it will also be denoted as an average over 'samples'). Finally, for a given realization of the disorder and a given configuration of the surface we also need to average over all origins $\boldsymbol{r}_0$ and all directions, all of these are denoted by the overbar.

It turns out that the same RSGM Hamiltonian also describes vortex arrays in two dimensions in the presence of weak point-like disorder. These are obtained when a magnetic field is applied parallel to a 2D film. This model was actually the first one for which the the existence of the vortex–glass transition was argued [5]. The variable $\phi(\vec{x})$ is related to the deviations of the flux lines from an ordered array of parallel straight lines with a distance b between them. Many of the recent theoretical studies of the RSGM were made in the flux-array context but clearly all conclusions apply equally to both systems. We should also mention that the same RSGM also describes a vortex-free XY model with a random field and some studies were made in this context.

The main analytical approaches, the renormalization-group [6] (RG) and the Gaussian variational [7, 8] (GV) method both predict a transition at the same critical temperature $T_c = \kappa/\pi$. The two methods also agree on the properties of the high temperature phase in which the discrete nature of the particle is irrelevant and the behaviour is that of the simple Gaussian model (without the cosine term in the Hamiltonian of (2.4)). For $T > T_c$ the correlation function is thus given by

$$C_0(\boldsymbol{r}) = \frac{T}{\kappa\pi} \, \ln |\boldsymbol{r}| \, . \tag{2.6}$$

The two approaches diverge in their predictions for $T < T_c$. RG calculations [3, 9–11] predict a new term with $\ln^2 |\boldsymbol{r}|$ which will dominate at large distances. To first order the RG calculations yield the following behaviour:

$$C(\boldsymbol{r}) = A \, C_0(\boldsymbol{r}) + B \, \tau^2 (\ln |\boldsymbol{r}|)^2 \tag{2.7}$$

where $\tau \equiv 1 - T/T_c$, A is a non-universal constant, and $B = 1/\pi^2 + \mathrm{O}(\tau)$ is a universal constant. Some other universal properties were found in [12].

The variational approach [7], the same scaling in $\ln|\boldsymbol{r}|$ as for $T > T_c$ is found for $T < T_c$ as well. The prefactor A, however, becomes T-independent and essentially remains at its value at T_c for the whole $T < T_c$ phase:

$$C(\boldsymbol{r}) = \frac{T_c}{\pi\kappa} \ln|\boldsymbol{r}| \,. \tag{2.8}$$

A similar calculation yields [8] $A(T)$ which increases at even lower temperature. The self-consistent Hartree approximation for the dynamics yields similar behaviour [13]. However, there are also subtle differences between the Hartree dynamics and the GV results in the regime of strong coupling where the transition is first order.

In a recent work the RG stability towards an *explicit* replica-symmetry breaking (RSB) was investigated [14]. It was found that for $T < T_c$ a small RSB term is relevant. However, this symmetry breaking does not occur spontaneously.

In another recent work, a variational approach without recourse to the replica trick was introduced [15]. All the GV results were reproduced under certain conditions but the connection between the two methods is not yet well understood.

Numerically, there is only a single paper in which the RSGM was addressed directly [16]. From a numerical simulation of the Langevin equation of motion derived from the weak coupling ($\lambda \ll 1$) RSGM no transition was found when the equilibrium properties were explored. When an applied force F was added a non-linear relation between the average velocity v and the F was found [16]. This is in qualitative agreement with the dynamical RG results [3].

The results presented below for the equilibrium behaviour will be clearly different from these simulations. However, it should be kept in mind that the surface model actually corresponds to the strong-coupling regime ($\lambda \sim 1$) of the RSGM (and, moreover, includes all harmonics with strength of order λ).

3. Numerical results and discussion

The simulations were performed on the CM computers of the Thinking Machines Corporation using the MC Metropolis algorithm. The moves, in which all the h_i of one sublattice are updated by increasing or decreasing them (independently) by one unit, are accepted or rejected following the Metropolis heat-bath algorithm.

We simulated, for every realization of the disorder, two copies (or replicas) of the system. They start each from different random initial conditions and each has its own time evolution but both surfaces have the same disordered substrate. This approach (introduced by Young in the spin-glass simulations [17, 18]) yields important information extracted from the overlaps of the two copies. In addition it allows an improved monitoring of when equilibration is achieved.

Measurement of the static quantities were taken only when equilibration was established. Data ('measurements') were taken over time intervals of the order of one or several equilibration time. The number of disorder realizations over which data was averaged varied between 100 and several thousands depending on the system size and the temperature. More details will be given below where specific calculations of different properties are addressed.

3.1. Height–height correlation function

Shugard *et al* [19] have performed the MC calculations of the discrete Gaussian model for a surface with a flat substrate. They confirmed the existence of the roughening transition

from a high-temperature rough phase (with a logarithmic behaviour of $C(\boldsymbol{r})$) and a flat low-temperature phase. To begin with we also simulated the pure model reproducing their results. Once the disorder was introduced the behaviour of $C(\boldsymbol{r})$ changed drastically in the low-temperature phase.

In figure 2 we show the general behaviour of the correlation function (2.5) for a pure and a disordered system. The simulations were performed for lattice sizes of $L = 64$ and 128. The values of $|\boldsymbol{r}|$ were taken to be up to $L/2$. The finite-size effects are reflected in the bending of $C(\boldsymbol{r})$ for large $|\boldsymbol{r}|$.

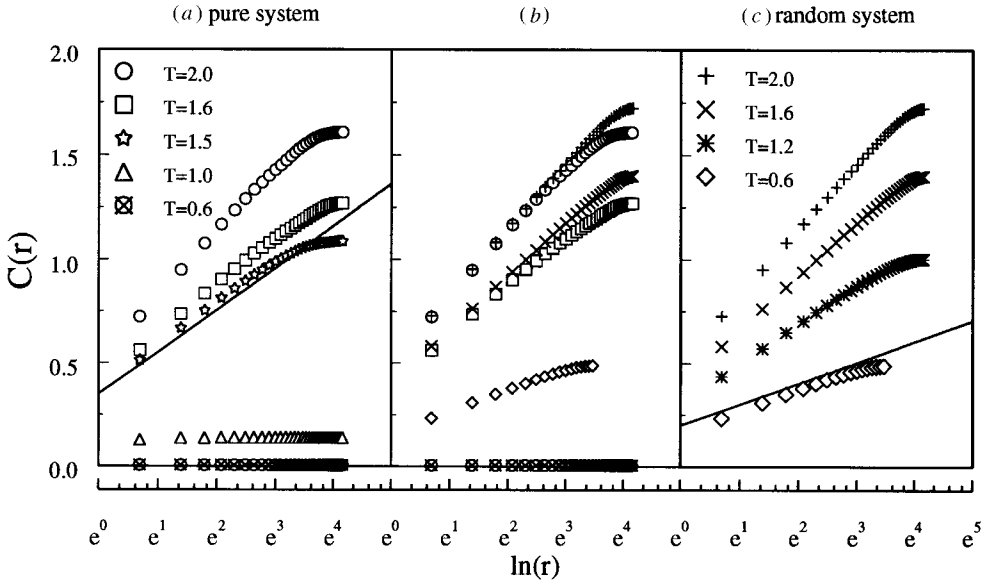

Figure 2. Semilog plot of $C(\boldsymbol{r})$ for different temperatures when: (*a*) disorder is excluded, (*c*) disorder is present and (*b*) overlap between these two cases. The straight line in (*a*) has slope $2/\pi^2$, while in (*c*) the slope is $1/\pi^2$.

Figure 2(*a*) shows the data obtained from simulations of the pure system at different temperatures. The full line is $C_0(\boldsymbol{r})$ (shifted by a constant independent of $\boldsymbol{r}$) at temperature $T_R \approx 1.45$ where the phase transition between the rough and smooth phases is expected to occur [19]. At the roughening temperature the slope assumes the universal value $2/\pi^2$. It can be clearly seen how the slope of $C_0(\boldsymbol{r})$ approaches this value as temperature decreases toward T_R. Below T_R the correlation function has some finite value independent of $|\boldsymbol{r}|$. The data for the disordered system are shown in figure 2(*c*). Now the full line has slope $1/\pi^2$ and was drawn at approximately the position where the phase transition is expected. The slope $1/\pi^2$ is the prediction of (2.7) and (2.8) at $T = T_c$. For clearer comparison, in figure 2(*b*) the previous two figures, the pure and disordered case, are superimposed on each other. For higher temperatures, the effect of the disorder is negligible. Lowering the temperature towards T_R, the difference becomes more apparent. (In the pure case, around T_R the slope behaves as $2/\pi^2 + c(T - T_R)^{1/2}$, where c is a non-universal constant.) Finally, below T_c the difference between the low-T behaviour of the pure and the disordered systems is obvious. Figure 3 shows a closer look at the behaviour of $C(\boldsymbol{r})$, for the disordered system, around the anticipated critical temperature $T_c = \kappa/\pi = 0.6366$ for our choice of $\kappa = 2$. In this case, the sample averaging was performed over 100 realizations. For each temperature,

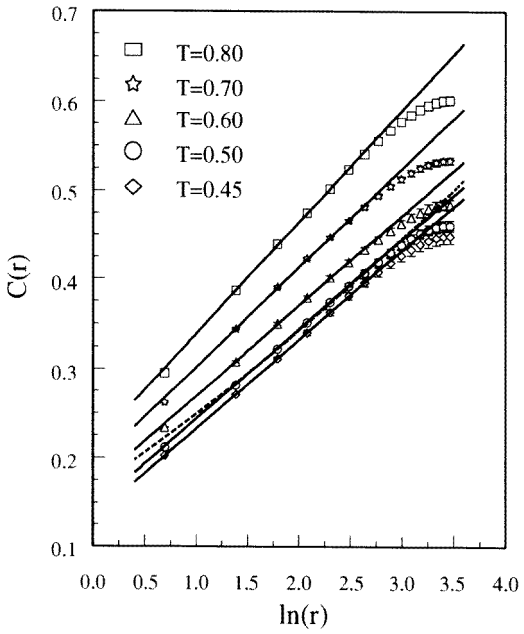

Figure 3. Semilog plot of $C(r)$ for $L = 64$. The straight lines are the best fits to $C(\boldsymbol{r}) = a(T) + b(T)\ \ln|\boldsymbol{r}|$. The broken curve is the RG prediction equation (2.7) at $T = 0.5$ with $A = 1$.

measurements were repeated, with a new set of 100 realizations of the disorder, five to ten times. The average values of these measurements with corresponding error bars are shown in figure 3.

We compare our results with both the renormalization-group predictions, equation (2.7), and with the results derived by the variational analysis with the one-step symmetry breaking scheme, equation (2.8). In both cases the theoretical results refer to the large-$|\boldsymbol{r}|$ behaviour of $C(\boldsymbol{r})$ while numerical results are always limited by the lattice size L and by finite-size effects.

According to the RG, equation (2.7), for T near T_c and for large $|\boldsymbol{r}|$ the effect of the second term, $B\tau^2 \ln^2|\boldsymbol{r}|$, should dominate. To compare with (2.7) we need to be close to T_c but not too close (since the coefficient is proportional to τ^2 and the distance $|\boldsymbol{r}|$ at which this term will dominate will be beyond the size of the system). We therefore choose $T = 0.5$ for the comparison. The broken curve shows (2.7) for that temperature and $A = 1$. It can be seen that the upper bending trend of the broken curve is for larger r less inconsistent with the MC data. The downwards bending of the MC points for each temperature (which was also observed in the data taken for the pure system) are due to the finite-size effects.

The replica variational approach predicts (see equation (2.8)) $C(\boldsymbol{r})$ to remain logarithmic for all T with a T-independent coefficient for $T \leqslant T_c$. The data shown in figure 3 are consistent with this behaviour. In our fit we used the values of the $C(\boldsymbol{r})$ for $|\boldsymbol{r}|$ between 4 and 14 lattice spacings. We neglected the higher values of $C(\boldsymbol{r})$ because of the presence of the finite-size effects as well as of strong sample to sample fluctuations. The full lines in figure 3 are the best-fit curves. In figure 4 we show the temperature dependence of the slopes for nine values of T between 0.45 and 0.9 including those in figure 3. The vertical dotted line $T = \kappa/\pi$ is the analytic result for T_c. While in the high-T phase the slope of $C(\boldsymbol{r})$ changes linearly with T, for the low-T phase it saturates around the value $1/\pi^2$ as is predicted by (2.8).

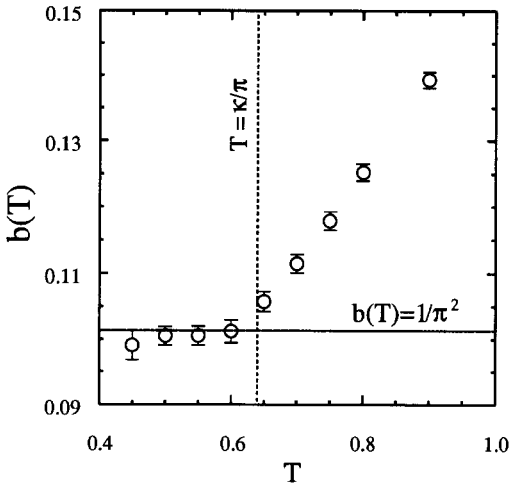

Figure 4. Plot of the coefficient $b(T)$ from the fitting equation $C(\boldsymbol{r}) = a(T) + b(T)\ \ln|\boldsymbol{r}|$. The vertical broken line is the analytic T_c. The horizontal line is the slope predicted by equation (2.8) for all $T \leqslant T_c$.

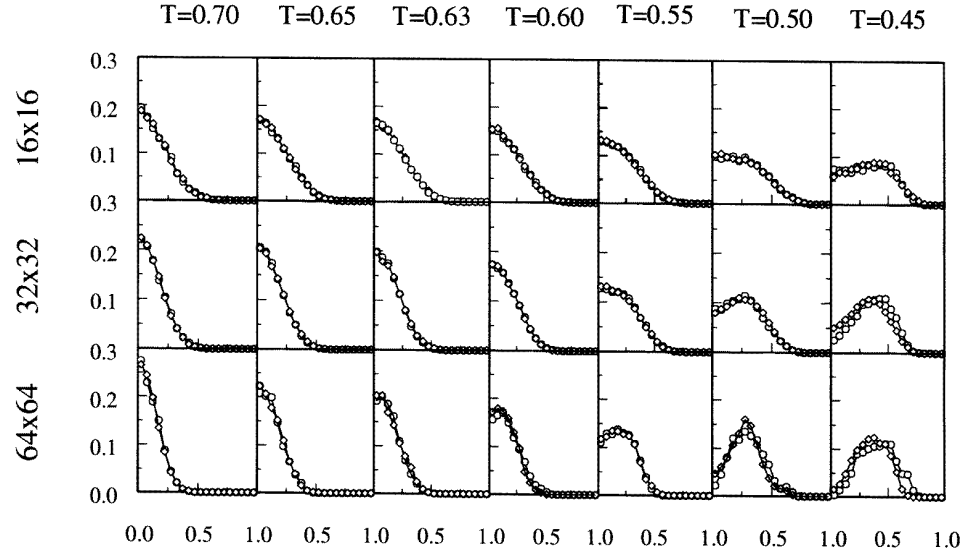

Figure 5. Plot of the suitable normalized probability distribution $P(|\tilde{q}|)$ for overlaps between the same replica at different time (circles) and different replicas at the same time (diamonds).

3.2. Autocorrelation function

To gain more insight into the transition and the properties of the low-temperature phase, a glassy order-parameter, its correlations, and/or probability distribution, should be invoked. The natural quantity to start with for the RSGM:

$$Q_{\alpha\beta}(\boldsymbol{r}, t) = \overline{\exp\left\{2\pi \mathrm{i}\left[h^{\alpha}(\boldsymbol{r}_0 + \boldsymbol{r}, t_0 + t) - h^{\beta}(\boldsymbol{r}_0, t_0)\right]\right\}} \tag{3.1}$$

cannot be used in the simulations of the discrete version of the model because

$$h^{\alpha}(\boldsymbol{r}_0 + \boldsymbol{r}, t_0 + t) - h^{\beta}(\boldsymbol{r}_0, t_0) = d(\boldsymbol{r}_0 + \boldsymbol{r}) - d(\boldsymbol{r}_0) + \text{integer} \tag{3.2}$$

and $Q_{\alpha\beta}$ is therefore constant.

Instead we tried to look at the local autocorrelation function:

$$q_i^{\alpha\beta}(t) = \left\{\left[h_i^{\alpha}(t_0+t) - \overline{h^{\alpha}(t_0+t)}\,\right]\left[h_i^{\beta}(t_0+\epsilon_{\alpha\beta}t) - \overline{h^{\beta}(t_0+\epsilon_{\alpha\beta}t)}\,\right]\right\} \tag{3.3}$$

where t_0 is time allowed for equilibration and the overbar means average over lattice sites. The replica indices α and β take values 1 or 2, and $\epsilon_{\alpha\beta} = 0$ if $\alpha = \beta$ or 1 if $\alpha \neq \beta$. This local quantity is first averaged over all sites:

$$q_{\alpha\beta}(t, t_0) = \frac{1}{N}\sum_{i=1}^{N} q_i^{\alpha\beta}(t) \tag{3.4}$$

where $N = L \times L$ is the total number of sites. This order-parameter definition includes the equal time overlap between different replicas as well as the auto-overlap of the same replica at different times.

The probability distributions $P(q_{\alpha\beta}, t_0)$ were calculated using

$$P(q_{\alpha\beta}, t_0) = \frac{1}{M}\left[\sum_{m=1}^{M} \delta\left(q_{\alpha\beta} - q_{\alpha\beta}(t_m)\right)\right]_{av} \tag{3.5}$$

where M is the number of measurements. When t_0 is longer than the longest relaxation time both distributions, for $\alpha = \beta$ and $\alpha \neq \beta$, tend to the equilibrium distribution, $P(q)$, defined by

$$P(q) = \left[\left\langle \delta\left(q - \frac{1}{N}\sum_{i=1}^{N}[h_i^{\alpha} - \overline{h^{\alpha}}\,][h_i^{\beta} - \overline{h^{\beta}}\,]\right)\right\rangle_T\right]_{av}. \tag{3.6}$$

The distribution $P(q)$ is Gaussian for $T > T_c$ but is expected to deviate from it for $T < T_c$. Clearly, at high temperature q goes to zero. On the other hand, at very low temperature the probability to change the surface height h_i is very small so that the crystal surface basically follows the disordered substrate. Trying to evaluate $q_{\alpha\beta}$ and g we could not reach enough accuracy to extract reliable results within the computer time available. A similar problem has been observed in simulations of the 3D Ising spin glass [18] and the 3D gauge glass [20]. One possible way out of this problem is to look for a quantity with similar scaling but for which statistical errors are smaller. The problem we have to overcome is that for T just below T_c the deviations from the Gaussian distribution occur first at very small values of q compared with its RMS. To accentuate the contribution from these small values we tried to evaluate the 'renormalized' quantity $\tilde{q}_{\alpha\beta}(t)$:

$$\tilde{q}_{\alpha\beta}(t) = \frac{\sum_{i=1}^{N} q_i^{\alpha\beta}(t)}{\sum_{i=1}^{N} |q_i^{\alpha\beta}(t)|}. \tag{3.7}$$

The distribution $P(\tilde{q})$ indeed exhibits a transition from a distribution with one maximum at $\tilde{q} = 0$ to a distribution with two maxima symmetric with respect to $\tilde{q} = 0$ (which becomes a local minimum). In figure 3 we show the suitable normalized distribution functions $P(\tilde{q})$ for different lattice sizes $L = 16$, 32, 64 and for seven values of T in the interval $T = 0.70$–0.45. Since the equilibrium distributions are symmetric, we only show $P(|\tilde{q}|)$. The sample averages were performed using 512, 256 and 100 samples for $L = 16$, 32 and 64, respectively. Depending on the temperature and the size of the simulated system, the MC runs were between 2^{15} to 2^{19} MC steps. The actual measurements were grouped into several groups, usually 8 or 16. Each inset shows the probability distribution of $|\tilde{q}|$ for $\alpha = \beta$ (circles) and $\alpha \neq \beta$ (diamonds) for some randomly chosen group of measurements averaged over samples. For the equilibrated system, the distribution of overlaps within the same replica and between the different ones should overlap as is seen in figure 3. Some

small deviation is noticeable for low T. It is worth mentioning that before the equilibration has been reached, the $P(|\tilde{q}|)$ as a function of time moves from left to right for $\alpha = \beta$ (because the two copies started from random uncorrelated states), and from right to left for $\alpha \neq \beta$ (for short times, the two copy states are strongly correlated [21]).

It is particularly interesting to look at the dimensionless combination of the moments:

$$g(T, L) = \frac{1}{2}\left\{3 - \frac{[\langle \tilde{q}^4_{\alpha\beta}\rangle_T]_{av}}{[\langle \tilde{q}^2_{\alpha\beta}\rangle_T]^2_{av}}\right\} \tag{3.8}$$

calculated after thermal equilibrium has been reached. The finite-size scaling ansatz for g is $\tilde{g}(L/\xi)$, i.e. for large enough size, L/ξ is the only relevant parameter. The RG approach [11] predicts $\xi \sim \exp(c/\tau^2)$. On the other side, if the transition is second order the expected finite-size scaling of g is: $g(T, L) \sim \tilde{g}(L^{1/\nu}(T - T_c))$ where ν is the correlation length exponent, $\xi \sim |T - T_c|^{-\nu}$. Therefore, at T_c curves of g for different system sizes L intersect one another. For the second-order transition, around T_c the curves have to splay out.

Our data for g are shown in figure 6. Depending on the temperature and the size of the simulated system, the MC runs for equilibration were between 2^{15} to 2^{19} MC steps. For smaller system size the average over disorder is performed using over 1000 samples. However, for large system size, $L = 64$, the equilibration time for temperatures below T_c is long, and we worked with a hundred samples. As in the calculation of $C(\boldsymbol{r})$, for each temperature the measurements were repeated several times. Again, the average values of these measurements with corresponding error bars are shown in figure 6. Clearly, figure 6 strongly suggests the existence of a phase transition somewhere in the temperature range 0.63–0.66. A finite-size scaling plot of g is shown in figure 7. The best fit is obtained with $T_c = 0.643 \pm 0.006$ and $\nu = 1.23 \pm 0.10$. The value of T_c is in good agreement with the analytic predictions discussed above.

Since g is dimensionless, its dynamical scaling form is given by $g(t) = G(t/\tau_0)$, where τ_0 is the relaxation time. If the transition is indeed second order, one expects a finite size scaling form $\tau_0(L, T) \sim L^z \tilde{\tau}_0(L^{1/\nu}(T - T_c))$, where z is the dynamical exponent [22]. At T_c this becomes $\tau_0(L, T_c) \sim L^z$, figures 8 and 9 show $g(t)$ as a function of the time t in MC steps and the scaled time t/L^z during its approach to the equilibrium value (≈ 0.18) at

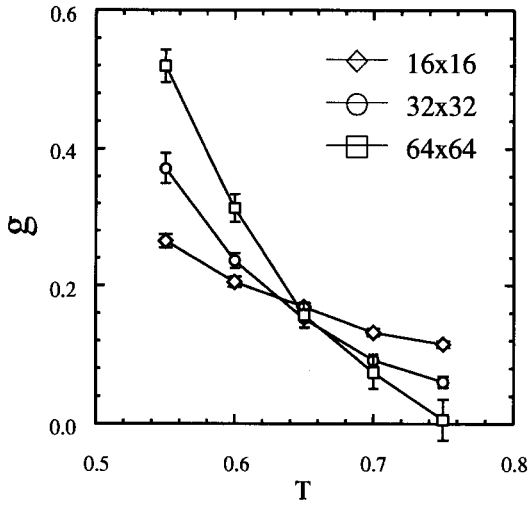

Figure 6. Plot of $g(T, L)$ against temperature T for different lattice sizes. The full lines are to guide the eye.

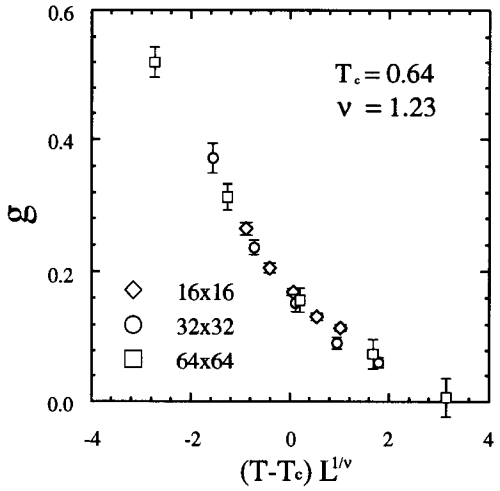

Figure 7. Finite-size plot of the data shown in figure 6 against the scaled variable with $T_c = 0.64$ and $\nu = 1.23$ (see the text).

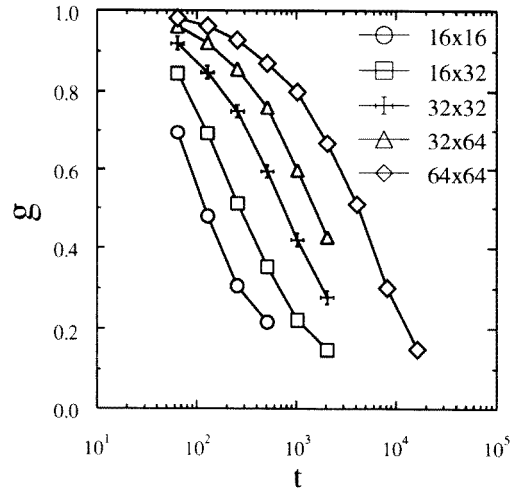

Figure 8. Plot of the $q(T_c, L)$ against time during the approach to the equilibrated configurations for different lattice sizes.

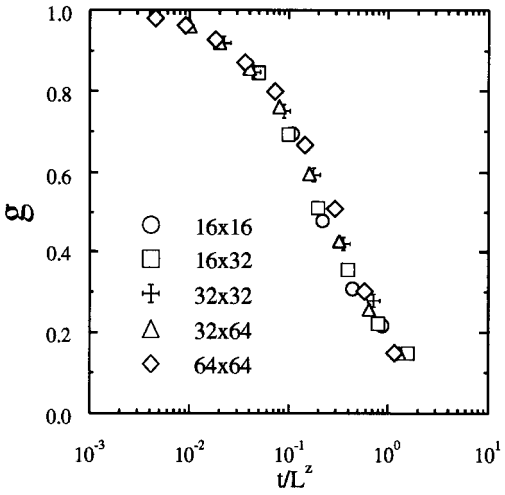

Figure 9. Plot of $g(T_c, L)$ at $T_c = 0.64$ against the scaled time $t/N^{z/2}$. The dynamical exponent z is 2.29.

$T = T_c$. During this time $g(t)$ is a highly fluctuating quantity and the average of the $g(t)$ over sufficiently many realizations of the disorder must be performed to obtain reproducible results. We used 16 384, 8192, 4096, 4096, 2048 realizations for system sizes of 16×16, 16×32, 32×32, 32×64, 64×64, respectively. The best fit gives $z = 2.29 \pm 0.16$ which is in a reasonable agreement with the expected theoretical value [3, 23], $z = 2$.

4. Conclusions

To summarize, the main results of this work are as follows:

(i) We verified the existence of a transition at $T_c \sim \kappa/\pi$ by inspecting the behaviour of two independent quantities: the height–height correlations and the overlap distribution $P(q)$ (directly and through the cumulant ratio $g(T, L)$). The only other numerical work, in which no transition was found in the behaviour of $C(\boldsymbol{r})$, was performed on the RSGM in the weak-coupling regime [16]. It may be that for weak coupling the scale at which the new behaviour takes over just below T_c is larger than the system size L that was investigated [24]. However, there is also an unlikely possibility that weak and strong coupling (to which our model belongs) are in distinct universality classes. It is also hard to see how such a scenario can be reconciled with the dynamic phase transition found in the same weak-coupling simulations.

(ii) We have found that the coefficient of $\ln|\boldsymbol{r}|$ dependence (which is proportional to T for $T > T_c$) saturates to a nearly constant value for $T < T_c$. The behaviour of this coefficient is consistent with the calculations of the GV approach [7] which predicts it to be constant below T_c (note that another GV calculation [8] and a self-consistent dynamical approach [13] predict that it will increase if the temperature is lowered well below T_c).

(iii) The histogram of $P(\tilde{q})$ shows that it changes from having a single maximum at $\tilde{q} = 0$ ($T > T_c$), to having two maxima at $\tilde{q} = \pm q^*$ for $T < T_c$. The form of $P(\tilde{q})$ does not show the form typical for one-step RSB (namely the existence of *two* maxima on either side of positive or negative $\tilde{q}$). On the other hand, the maximum is so broad that we cannot rule out the existence of two maxima. Simulations of larger size samples will make the features of $P(\tilde{q})$ sharper such that the two possibilities might be distinguishable.

(iv) From the cumulant ratio $g(T, L)$ we could provide the first estimate for the correlation length exponent $\nu \approx 1.23$. Note that a power-law behaviour of the correlation length is in disagreement with variational calculations and the RG. In both theories the correlation length diverges exponentially: $\xi \sim \exp(c/\epsilon^2)$ from RG calculations and $\xi \sim \exp(c'/\epsilon)$ from GV and a dynamic Hartree approximation. Clearly more analytic work on the issue of whether the transition is second or infinite order will be worthwhile.

(v) The slowing down of the transition yields a rough estimate for the dynamic exponent $z \approx 2.29 \pm 0.16$.

After this work was completed two new numerical works were reported in recent preprints. In [24] the RSGM was simulated directly on a lattice for different strength of coupling λ. Its results confirm the ones presented above for strong λ. For weaker λ it demonstrates that one needs larger $|\boldsymbol{r}|$ to observe the saturation of the coefficient A to a temperature independent value. The temperature-dependent term $C_0(\boldsymbol{r})$ dominates on a shorter scale when λ is small. That partly explains the lack of transition observed in [16].

In another paper [25], simulations of the random-substrate surface similar to the one reported above, were carried by another group. The simulated systems were larger by a factor of two. Their results agree with those presented here but they were given a different interpretation. They used the exact $C_L^0(\boldsymbol{r})$ for a finite lattice of size L and found the best fit when a term $[C_L^0(\boldsymbol{r})]^2$ was included below T_c. The coefficient of this term is about one

fifth of the RG prediction. We have analysed our data following this interpretation and the results are consistent (within the error bars) with the ones found in [25]. It should also be noticed that such behaviour may be explained within the GV approach due to the crossover (mentioned above) from C_L^0 at small $|\boldsymbol{r}|$ to the temperature-independent behaviour, which has a higher slope, at large $|\boldsymbol{r}|$. These last two works have made important contributions to the debate but at the same time they demonstrate that it is still far from reaching its conclusion.

Acknowledgments

We are very grateful to T Giamarchi, T Hwa, and Y-C Tsai for most useful discussions. We also thank Thinking Machines Corporation for use of their computers. Acknowledgment is also made to the donors of The Petroleum Research Fund, administrated by the ACS, for support of this research. This research was supported in part by the National Science Foundation under grant no PHY89-04035.

References

[1] Chui S T and Weeks J D 1976 *Phys. Rev.* B **14** 4978; *Phys. Rev. Lett.* **40** 733
[2] Nozieres P and Gallet G 1987 *J. Physique* **48** 353
[3] Tsai Y-C and Shapir Y 1992 *Phys. Rev. Lett.* **69** 1773; 1994 *Phys. Rev.* E **50** 3546
[4] Cule D and Shapir Y 1995 *Phys. Rev. Lett.* **74** 114
[5] Fisher M P A 1989 *Phys. Rev. Lett.* **62** 1415
[6] Cardy J L and Ostlund S 1982 *Phys. Rev.* B **25** 6899
[7] Giamarchi T and Le Doussal P 1994 *Phys. Rev. Lett.* **72** 1530
[8] Korshunov S E 1993 *Phys. Rev.* B **48** 3969
[9] Goldschmidt Y Y and Houghton A 1982 *Nucl. Phys.* B **210** 115
[10] Villain J and Fernandez J F 1984 *Z. Phys.* B **54** 139
[11] Toner J and DiVincenzo D P 1990 *Phys. Rev.* B **41** 632
[12] Hwa T and Fisher D S 1993 *Phys. Rev. Lett.* **72** 2466. Note that $B = 2/\pi^2$ was obtained there and corrected later (T Hwa Private communication)
[13] Cule D and Shapir Y 1995 *Phys. Rev.* E **51** 3305; and unpublished
[14] Le Doussal P and Giamarchi T 1995 *Phys. Rev. Lett.* **74** 606
[15] Orland H and Shapir Y 1995 *Europhys. Lett.* **30** 203
[16] Batrouni G G and Hwa T 1994 *Phys. Rev. Lett.* **72** 4133
[17] Young A P 1983 *Phys. Rev. Lett.* **51** 1206
[18] Bhatt R N and Young A P 1985 *Phys. Rev. Lett.* **54** 924; 1988 *Phys. Rev.* B **37** 5606
[19] Shugard W J, Weeks J D and Gilmer G H 1978 *Phys. Rev. Lett.* **41** 1399
[20] Reger J D 1992 *Computer Simulation Studies in Condensed Matter Physics V* ed D P Landau, K K Mon and H B Schüttler (Berlin: Springer)
[21] Bhatt R N and Young A P 1988 *J. Phys. C: Solid State Phys.* **21** L57
[22] Bhatt R N and Young A P 1992 *Europhys. Lett.* **20** 59
[23] Goldschmidt G G and Schaub B 1985 *Nucl. Phys.* B **251** 77
[24] Rieger H 1995 *Phys. Rev. Lett.* **74** 4964
[25] Marinari E, Monasson R and Ruiz-Lorenzo J J 1995 *J. Phys. A: Math. Gen.* **28** 3975